

Circular Kinks on the Surface of Granular Material Rotated in a Tilted Spinning Bucket

Sangsoo Yoon^{1,2}, Byeong-ho Eom^{1,2}, Jysoo Lee¹ and [†]Insuk Yu^{1,2}

Department of Physics¹ and Condensed Matter Research Institute²

Seoul National University, Seoul 151-742, Korea

Abstract

We find that circular kinks form on the surface of granular material when the axis of rotation is tilted more than the angle of internal friction of the material. Radius of the kinks is measured as a function of the spinning speed and the tilting angle. Stability consideration of the surface results in an explanation that the kink is a boundary between the inner unstable and outer stable regions. A simple cellular automata model also displays kinks at the stability boundary.

PACS number: 46.10.+z, 47.20.Ma, 47.54.+r, 81.05.Rm]

Granular materials behave differently from any other familiar forms of matter. They possess both solid- and fluid-like nature and exhibit unusual dynamic behaviors, such as segregation, surface waves, heap formation and convection [1–5]. The surface of granular material in a spinning bucket is an example of such interesting phenomena. Vavrek and Baxter [6] showed that the surface shape of sand in a vertical spinning bucket can largely be explained using Coulomb’s criterion. Medina *et al.* [7] investigated hysteresis of the surface shape with semi two-dimensional rotating bins and showed the existence of multiple steady-state solutions. Yeung [8] studied the system with an initially conical surface. By using a model of granular surface flow [9,10], he found that the behaviors of the model agreed well with the experiments.

When we tilt the rotational axis of a bucket from the vertical direction, circular kinks develop on the granular surface if the tilting angle is greater than the angle of internal friction of the material. A glass beaker of 10.5 cm diameter and 1 liter capacity is used as a spinning bucket. The beaker is mounted on a dc motor to rotate around its axis of symmetry. The motor is fixed to a stand such that the tilting angle α can be varied. The rotation rate is varied from 0 to 300 rpm by controlling the voltage. The angular velocity ω is measured by using a photogate timer and is constant within an error smaller than 1 rpm. We use natural sand, as used in general construction, as a prototypical granular material. In order to insure the monodispersity of sands, two sieves with 0.35 and 0.25 mm meshes are used and the sizes in between are selected. The angle of internal friction (angle of repose) and apparent density are found to be $\theta_f = 34 \pm 1^\circ$ and $\rho = 1.52 \text{ g/cm}^3$, respectively.

Figure 1(a) is a schematic side-view and 1(b) is a top-view photograph of a circular kink formed on the sand surface. To measure the diameter of the kinks, a divider is placed near a kink and matched with the diameter. Several measurements are carried out for each kink and errors of measurements are about 1 mm. We also measure the surface shapes in some cases using the method of Ref. 6.

First, we tilt the bucket by angle α and then turn on the motor to various speeds.

In this type of experiment the initial granular surfaces are inclined flat surfaces. After a few minutes of rotation, we measure the radius of kinks r_k . The radius depends on ω as $r_k \propto \omega^{-2+x}$ ($-0.2 \leq x \leq 0.1$), thus a dimensionless radius $R_k = r_k \omega^2 / g$, which is roughly constant, can be introduced (Fig. 2). Next, the tilting angle is varied at fixed ω . When $\alpha \leq 30^\circ$, there forms a paraboloid-like granular surface whose shape depends on the initial condition but does not change with time. As α becomes larger than about 35° , a circular kink forms which is independent of the initial granular surface. Inside the kink, most of the grains on the surface avalanche during the rotation and we can see a complex motion like a whirlpool. The surface shape of the inner region is asymmetric about the rotation axis. On the other hand, those grains at and outside the kink are stationary with respect to the bucket. The surface shape of the solid-like region is in general asymmetric and depends on the initial surface. However, when we first rotate the bucket vertically with an initially conical surface and then tilt slowly, the surface shape remains nearly symmetric. The kink is a boundary between the two dynamically distinguishable regions. As α increases, the R_k tends to increase. The measured values of R_k at several tilting angles are shown in Fig. 3. For $\alpha > 70^\circ$, a new type of instability appears; some sand grains are separated from the surface and fall freely during the rotation.

We also study hysteresis by sequentially increasing, decreasing or randomly changing the angular velocity. For fixed α , the radius of kinks is determined only by ω and does not depend on the past history of changing ω . But the shape of the surface shows hysteresis. When ω increases a new kink appears inside the previous one. The previous kink formed at slower ω can be frozen in the solid-like outer region. Thus, there can be many concentric kinks. On the other hand, when ω decreases a new kink appears outside the previous one and the previous kinks are always washed out.

Various vessels are tested as spinning buckets. If the width of a container is larger than the diameter of a kink, the radius of the kink does not depend on the size or shape of the container. We find that, to form the kinks, it is not necessary for the rotational axis to coincide with the axis of symmetry of a container. When we rotate a rectangular box

around an axis which is fixed on one of the side-walls, there appears a semicircular kink.

Similar kinks are also found with the silica-gel (Matrex Silica, Amicon Corp., Danvers, MA 01923, U.S.A., of apparent density $\rho = 0.35 \text{ g/cm}^3$, particle diameter around 0.2 mm, and the angle of internal friction $\theta_f = 30 \pm 1^\circ$), but the R_k 's are smaller by about 20 % than with the sand. We try sugar powder (sucrose, grain size $\sim 0.2 \text{ mm}$, after 100°C for 2 hours to remove moisture), and observe kinks too.

We now discuss the stability of the granular surface. There are four forces acting on a grain at the surface in the rotating frame: gravity $m\vec{g}$, centrifugal force $m\vec{r}\omega^2$, normal force \vec{N} and frictional (shearing) force \vec{f} . Here, m is the mass of a grain, \vec{g} the gravitational acceleration and \vec{r} is the radial displacement of the grain from the rotational axis. We make the following assumptions. First, there is no bulk motion in the pile and the grain at the surface can only slide or roll on the surface. Second, there is no inertial effect. The grain stops as soon as it satisfies a force balance equation. Third, we also assume the Coulomb yield condition [6,11], which states that the grain does not move when $f \leq \mu N$, where μ ($\mu = \tan \theta_f$) is the coefficient of friction. The force balance equation for the granular system is

$$\vec{N} + m\vec{g} + m\vec{r}\omega^2 + \vec{f} = 0, \quad f \leq \mu N. \quad (1)$$

We define a dimensionless vector

$$\vec{n}_h = - \frac{m\vec{g} + m\vec{r}\omega^2}{mg}, \quad (2)$$

which is normal to the stable surface when there is no friction ($\vec{f} = 0$). The inclination of the rotational axis breaks the cylindrical symmetry of the vector \vec{n}_h and makes the angle β between \vec{n}_h and \hat{z} time-dependent, where β is also the angle between the stable surface without friction and the bottom plane of the spinning bucket (Fig. 4).

The kink is an abrupt change in the slope of the granular surface along the radial direction. Therefore, we concentrate on the radial motion of grains. The radial stability condition can be expressed in terms of the angle β

$$\tan(\beta(t) - \theta_f) \leq \tan \theta \leq \tan(\beta(t) + \theta_f), \quad (3)$$

where $\tan \theta$ is the local slope of the granular surface in the radial direction with respect to the bottom of the bucket (Fig. 4).

The stable surface satisfying Eq. (3) for all t , can exist only if the following condition is satisfied;

$$\beta_{\max} - \theta_f \leq \beta_{\min} + \theta_f, \quad (4)$$

where β_{\max} (β_{\min}) is the maximum (minimum) value of $\beta(t)$ during rotation. If we use a cylindrical coordinate system (ρ, ϕ, z) aligned to the rotation axis, the \vec{n}_h and $\beta(t)$ can be expressed as

$$\vec{n}_h = \hat{\rho}(\sin \alpha \sin \phi - R) + \hat{\phi} \sin \alpha \cos \phi + \hat{z} \cos \alpha \quad (5)$$

and

$$\cos \beta(t) = \frac{\cos \alpha}{\sqrt{R^2 + 1 - 2R \sin \alpha \sin \omega t}}, \quad (6)$$

where $R = r\omega^2/g$ is a dimensionless radius and $\phi = \omega t$ (the phase is chosen that $\phi = \pi/2$ corresponds to the highest position during rotation). The β_{\max} (β_{\min}) in Eq. (4) becomes the angle $\beta(t)$ at $\phi = 3\pi/2$ ($\phi = \pi/2$).

Finally, we reach the following radial stability condition,

$$R \geq \begin{cases} 0 & (\alpha \leq \theta_f) \\ R_c \equiv \sqrt{\frac{\sin 2(\alpha - \theta_f)}{\sin 2\theta_f}} & (\alpha > \theta_f). \end{cases} \quad (7)$$

If $\alpha \leq \theta_f$, the steady state surface is stable for all R . If $\alpha > \theta_f$, the surface can be stable only in the region where R is larger than the critical radius R_c . In the region with smaller R , avalanches of grains occur. We plot the $R_c(\alpha)$ in Fig. 3 for the sand sample with $\theta_f = 34^\circ$ to compare with the radius of kink. The critical radii calculated by Eq. (7) reflect the qualitative features of the experimental kink radius; they increase with the inclination angle and do not depend on the angular velocity.

The angular stability condition is also examined. The corresponding critical radius R_c^ϕ for the azimuthal direction is always larger than R_c , and their difference increases monotonically as α increases. In our experiment ($35^\circ \leq \alpha \leq 70^\circ$), however, the difference is small and the angular instability is expected to have little effect on the formation of kinks.

In order to gain insights on the formation of the kinks, we study the system using a simple cellular automata model similar to that of Bak *et al.* [12,13]. In addition to the assumptions made earlier, we further assume that the relative motion of grains in the azimuthal direction is not significant. Experimentally, grains just inside the kink show nearly circular trajectories without relative movement in the azimuthal direction. Since the kinks are formed by the motion of grains nearby the kinks, we expect that the above assumption does not alter their formations. The two-dimensional granular surfaces can now be described by one-dimensional curves—the surface profile $h(R)$ at a given ϕ .

The spatial coordinate R is made discrete—it is replaced by $R_i = i \Delta R$ ($i = -n, -n + 1, \dots, n$), which runs from one end of the container to the other end. We measure local slopes s_i , defined as $(h(i) - h(i + 1))/\Delta R$, and check the stability of all the slopes following the criterion of Eq. (3). We then update the heights of the pile to make the local slopes at least marginally stable starting from the uphill and proceeding towards the downhill.

If the local slope s_{i-1} becomes unstable due to an update at the i -th site, we allow “backward propagation”, where a perturbation at a site can influence a site uphill from the perturbation. To be more specific, we decrease the height $h(i - 1)$ and transfer the excess amount to the $(i + 1)$ th site. If the change makes the $(i - 2)$ th site unstable, its height is decreased in a similar way. We proceed until all local slopes become stable. Then the container is rotated by a small angle $\delta\phi$ and we again update the height. For computational simplicity we assume that the relaxation time of the pile is much shorter than the period of the rotation. At the boundary, we apply a mass conservation condition; grains cannot enter nor leave the container.

In Fig. 5, we show time evolutions of the heights $h(i, t)$ with different initial conditions

plotted during a half rotation. Here, $\Delta R = 0.01$, $\alpha = 45^\circ$, $\theta_f = 34^\circ$, and $\delta\phi = \frac{\pi}{3} \times 10^{-2}$ rad. One can see the region with large $|R|$ is solid-like; the profile does not change with time. On the other hand, the inner region is fluid-like; the heights keep changing. There is a discontinuity in the slope at the border of the two regions ($|R| \simeq 1.2$). The resulting kink looks similar to what is observed in the experiments. Although the formation of the kinks does not depend on the initial surface, the profile of the solid-like region does. The radii $R_k(\alpha)$ resulting from the simulation with $\theta_f = 34^\circ$ are shown in Fig. 3 for different α in the range ($0^\circ - 90^\circ$). One notices that not only the qualitative features such as the threshold angle ($\alpha = \theta_f$) and the overall shape, but also their numerical values are in good agreement with the measured ones. However, this quantitative agreement may be accidental, since we expect the present simple model to reproduce qualitative, but not quantitative behaviors. To study the hysteresis behaviors, we start with a kink formed on the surface at $\alpha = 40^\circ$, and suddenly increase α to 65° . There indeed appears a new kink with smaller radius, leaving the old one stable, similar to what is observed in the experiments.

Finally, the formation of the kinks can be viewed as follows. Consider the border at R_c from the stability analysis. There will be avalanches just inside the border. Due to the backward propagation, which we expect to exist in real sandpiles, the region just outside the border should be involved in the avalanche. This explains why the measured R_k is larger than R_c as shown in Fig. 3. The surface in the stable region will be marginally stable, so we expect its slope is a smooth function of R . The surface in the inner unstable region, however, is produced by a process different from that for the surface outside the border, so there is no reason to expect that the two slopes join smoothly. It is thus natural to expect that a sudden change in the slope is observed at the border between the solid-like and fluid-like regions.

In summary, we have discovered circular kinks on the surface of granular material in a spinning bucket when its axis of rotation is tilted beyond the angle of internal friction. The radius of the kinks depends on the angular velocity, the tilting angle and the angle of internal friction. With a fixed tilting angle, the dimensionless radius of kinks $R_k = r_k \omega^2 / g$ remains

roughly constant. We find that the surface is divided into two regions: a fluid-like inner and a solid-like outer regions. We determine the critical radius R_c from the radial stability condition and the prediction reflects the basic features of the experiments. Using a simple cellular automata model, with the same stability condition and by allowing the propagation effect of avalanche, we obtain the granular surface in good accord with the experiments.

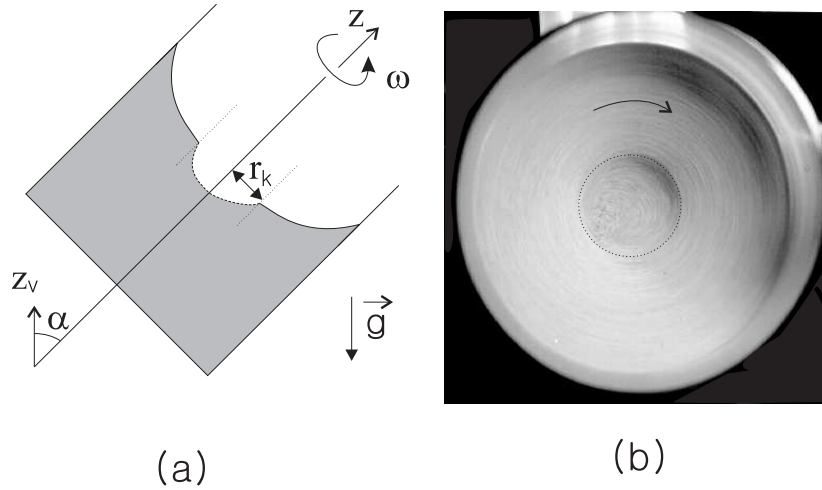
This work is supported by the Basic Science Research Institute, Seoul National University and by Korea Science and Engineering Foundation (KOSEF) through the Science Research Center for Dielectrics and Advanced Matter Physics. One of us (J.L.) is supported in part by KOSEF through the Brain-pool program and SNU-CTP.

[†]Electronic address : isyu@snu.ac.kr

REFERENCES

- [1] H.M. Jaeger, S.R. Nagel, and R.P. Behringer, *Rev. Mod. Phys.* **68**, 1259 (1996).
- [2] H. Hayagawa, H. Nishimori, S. Sasa, and Y-h. Taguchi, *Jpn. J. Appl. Phys.* **34**, 397 (1995).
- [3] A. Mehta, *Physica A* **186**, 121 (1992).
- [4] R. Behringer and J. Jenkins, eds., “Powders & Grains '97” (Balkema, Rotterdam, 1997).
- [5] C.S. Campbell, *Ann. Rev. Fluid Mech.* **22**, 57 (1990).
- [6] M.E. Vavrek and G.W. Baxter, *Phys. Rev. E* **50**, R3353 (1994).
- [7] A. Medina, E. Luna, R. Alvarado, and C. Trevino, *Phys. Rev. E* **51**, 4621 (1995).
- [8] C. Yeung, *Phys. Rev. E* **57**, 4528 (1998).
- [9] J.-P. Bouchaud, M.E. Cates, J.R. Prakash, and S.F. Edwards, *Phys. Rev. Lett.* **74**, 1982 (1995).
- [10] A. Mehta, J.M. Luck, and R.J. Needs, *Phys. Rev. E* **53**, 92 (1996).
- [11] R. Jackson, in R. Meyer, ed., *The Theory of Dispersed Multiphase Flow* (Academic Press, New York, 1983).
- [12] P. Bak, C. Tang, and K. Wiesenfeld, *Phys. Rev. Lett.* **59**, 381 (1987).
- [13] P. Bak, C. Tang, and K. Wiesenfeld, *Phys. Rev. A* **38**, 364 (1988).

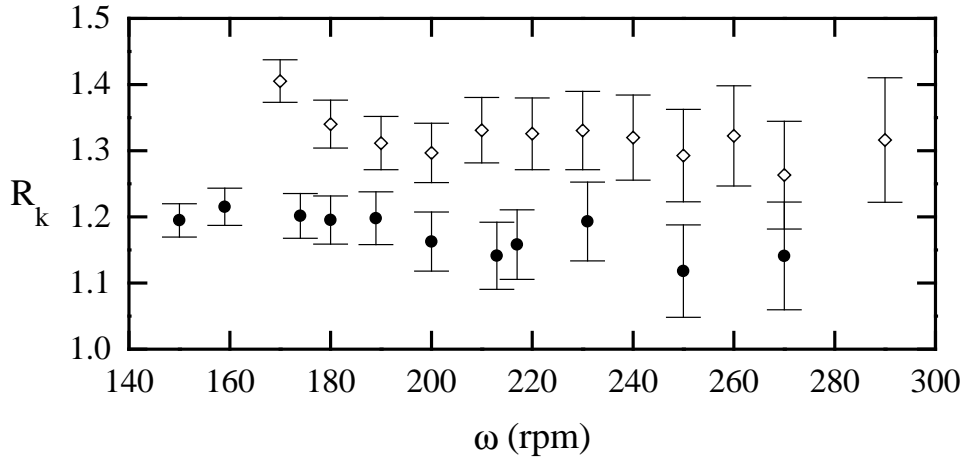
Fig. 1



Yoon et al.

FIG. 1. (a) Schematic side-view of a tilted spinning bucket: the rotational axis z is tilted from the vertical direction z_v by an angle α . A kink of radius r_k forms on the granular surface separating the solid-like (profile stable) outer region from the fluid-like (profile unstable) inner region. \vec{g} denotes the gravity. (b) Top-view photograph of a kink formed on the sand surface (stressed by a dotted circle, of radius 2.0 cm, for a clearer view) rotated with $\omega = 230$ rpm (direction is indicated by an arrow) and $\alpha = 45^\circ$.

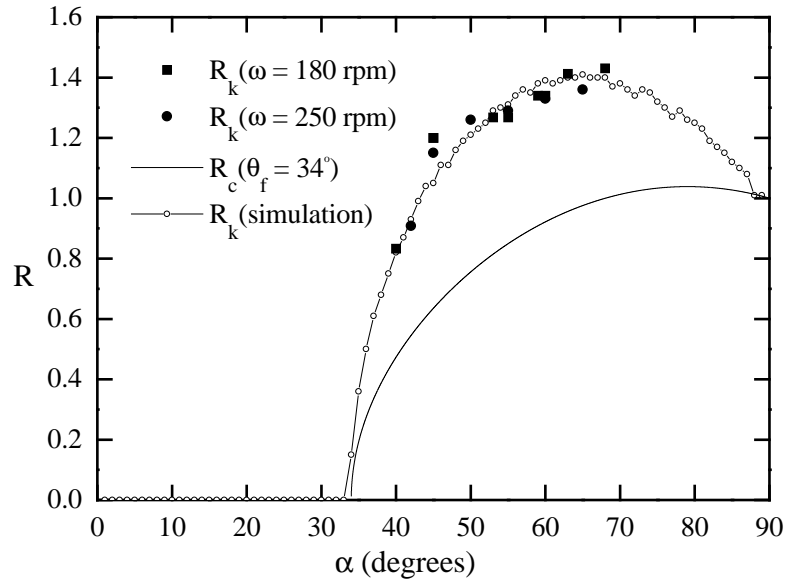
Fig. 2



Yoon et al.

FIG. 2. The dimensionless radius $R_k = \frac{r_k \omega^2}{g}$ of the kinks formed on the sand pile. Examples for the two tilting angles, $\alpha = 60^\circ$ (\diamond) and $\alpha = 45^\circ$ (\bullet), indicate the relation $r_k \propto \omega^{-2}$. Errors of the measurements are $\Delta r_k \simeq 1$ mm.

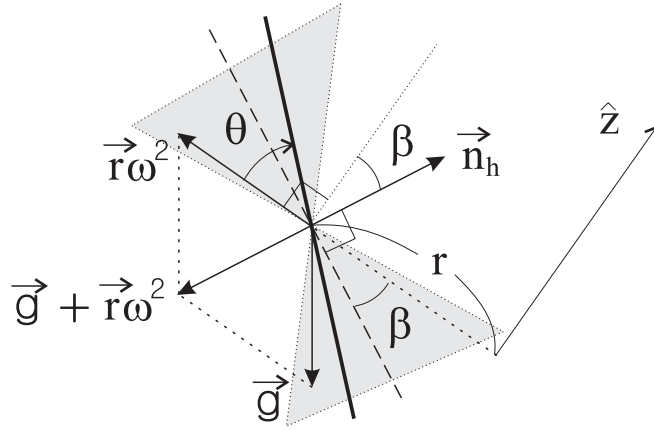
Fig. 3



Yoon et al.

FIG. 3. The dimensionless radius R_k for sand at various α . Representative data for two values of ω are shown together with the critical radius R_c (—) calculated for stability and the R_k from simulation (— o —) with the angle of internal friction (angle of repose) $\theta_f = 34^\circ$.

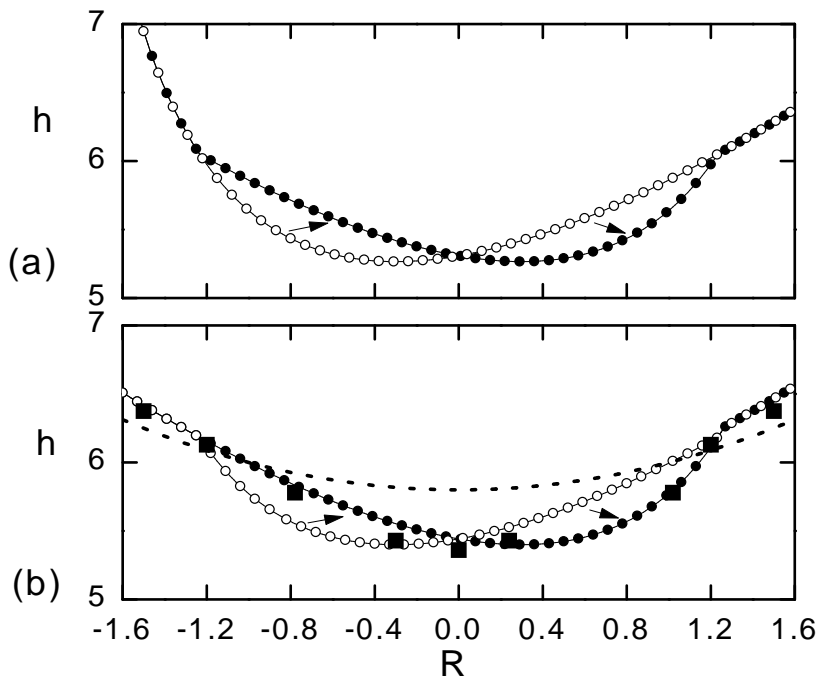
Fig. 4



Yoon et al.

FIG. 4. The vector \vec{n}_h is normal to the local surface (dashed line) when there is no friction. The angle β between the vector \vec{n}_h and the rotation axis \hat{z} is changing during rotation. The granular surface (solid line) in the shaded region is stable for the angle θ between the granular surface and bottom of the bucket in the range $\beta - \theta_f \leq \theta \leq \beta + \theta_f$, where θ_f is the angle of repose. This figure is an example that a grain is at the top position during rotation.

Fig. 5



Yoon et al.

FIG. 5. Time evolutions of the granular surface calculated from the simulation of a simple cellular automata model with $\theta_f = 34^\circ$ and $\alpha = 45^\circ$ for two different initial conditions; (a) first tilt and then rotate, (b) first rotate vertically and then tilt slowly. Different initial preparations give different surface profiles, which however result in the same radii of kinks. The open and filled circles indicate the surface profiles at the initial and after a half (π -radian) rotation positions, respectively, and two arrows represent the direction of changes. In (b), the filled squares are the experimental data, which are scaled by $\frac{\omega^2}{g}$, and the dashed line is the parabolic best fit to the data in the solid-like region ($1.2 < |R| < 4$). The experimental data in the fluid-like region ($|R| < 1.2$) are only rough estimates ($\Delta h \simeq 0.2$) due to the steady flow of grains. The data at $R > 0$ correspond to the upper half of the granular surface.